Plastic shrinkage and cracking risk of recycled aggregates concrete

Ahmed Bendimerad, Emmanuel Rozière, Ahmed Loukili

▶ **To cite this version:**

Ahmed Bendimerad, Emmanuel Rozière, Ahmed Loukili. Plastic shrinkage and cracking risk of recycled aggregates concrete. Construction and Building Materials, 2016, 121, pp.733-745. ⟨10.1016/j.conbuildmat.2016.06.056⟩. ⟨hal-05406596⟩

HAL Id: hal-05406596

https://hal.science/hal-05406596v1

Submitted on 2 Jan 2026

HAL is a multi-disciplinary open access archive for the deposit and dissemination of scientific research documents, whether they are published or not. The documents may come from teaching and research institutions in France or abroad, or from public or private research centers.

L'archive ouverte pluridisciplinaire **HAL**, est destinée au dépôt et à la diffusion de documents scientifiques de niveau recherche, publiés ou non, émanant des établissements d'enseignement et de recherche français ou étrangers, des laboratoires publics ou privés.

Distributed under a Creative Commons CC BY-NC 4.0 - Attribution - Non-commercial use - International License

Plastic shrinkage and cracking risk of recycled aggregates concrete

Ahmed Z. Bendimerad, Emmanuel Rozière, Ahmed Loukili *

Civil Engineering and Mechanics Research Institute (GeM) – UMR CNRS 6183, Ecole Centrale de Nantes, 44321 Nantes, France

This paper presents the results of experimental research on recycled concrete at early age. The influence of recycled gravel and sand (RG and RS) and initial water saturation of RG on plastic shrinkage and crack ing sensitivity was investigated. Four initial water saturations were studied: 30%, 70%, 100% and 120% of saturated surface dried (SSD). The total water was kept constant for all the mixtures, so the added water was adjusted to take into account the absorption of the aggregates during the mixing process. Other con crete mixtures were designed using 30% and 100% of recycled gravel, and 30% of recycled sand. The gravel/sand ratios were adjusted to keep the maximum paste thickness (MPT) constant. To understand the evolution of early age parameters, a timeline was established and the analyses showed correlations between the evolution of plastic shrinkage and other properties at early age. The initial water saturation did not significantly affect the evolution of plastic shrinkage. Recycled aggregates actually show a rela tively high rate of absorption during the first hour after mixing, i.e. before the development of plastic shrinkage. A stress/strength approach based on experimentally assessed parameters was used to compare the cracking sensitivity of different concretes with recycled aggregates. A high rate of substitution of recycled gravel or sand affected the early age properties of the recycled concrete and the cracking sensi tivity especially when natural sand was replaced by recycled concrete sand.

1. Introduction

The extraction of construction materials grew by a factor of 34 during the twentieth century [1]. The global material extraction of construction minerals now represents more than 10 billion tons per year [2], which means approximately 1.5 t/cap/yr. Sustainable development has become a strategic issue and affects construction materials in terms of CO_2 emission, energy consumption and the use of natural raw materials. The changes towards a more sustain able economy require a reduction in resource use at a global level. Most of the environmental impacts of extraction and use of con struction minerals occur at a regional level. All extraction activities of these materials cause damages to land, air and water ecosystems. Furthermore, energy use for extraction and transport needs to be considered. Similarly, a large part of the processing involves the production of concrete, which involves cement that is a major source of CO_2 emissions. Extractive operations often gen erate large volumes of waste; similarly, at the end of the life cycle high volumes of waste require disposal [3]. Therefore, many Euro pean countries have introduced new charges and taxes to reduce the demand for primary materials and encourage recycling [4]. In many urban areas, a critical shortage of natural aggregates is detected. At the same time, increasing quantities of demolished concrete from old structures are generated as waste material in these same areas.

The use of construction and demolition waste obtained from building demolition as recycled aggregates for the production of new concrete has become more common for the last decade. How ever, the influence of aggregates on short term and long term

* Corresponding author.
E-mail address: ahmed.loukili@ec-nantes.fr (A. Loukili).

Accepted Manuscript

behaviour of concrete is significant [5 6]. Particle size distribution, shape, porosity (measured as water absorption), and initial water saturation affects workability, plastic stage properties, setting and hardening, strength, durability and time dependent behaviour shrinkage and creep. Generally, the absorption at 24 h [7] is taken as a reference to assess effective water and added water contents. However, setting of cement paste may occur before the full absorp tion of water by aggregates. Thus, the actual water content of cement paste is not the theoretical content and the water/cement ratio is modified. Therefore, the behaviour of concrete is influenced by the properties and the initial water saturation of aggregates.

According to Powers [8] plastic shrinkage may occur when the evaporation rate exceeds the bleeding rate. Early age cracking of horizontal concrete elements is likely to appear a few hours after it is cast, during setting and early hardening of concrete. The con crete cracking phenomena depend on several parameters, such as the magnitude and kinetics of shrinkage, the evolution of tensile strength or tensile strain capacity [9], the stiffness and the relax ation of the material. Two methods can be found in literature for analyzing the cracking sensitivity. The first one is based on the strain capacity [10 11] and the second on stress criteria [12 13]. On the other hand, the ACI [14] and other researchers [15 16] indi cate a higher cracking risk when the deformation at early age exceeds the threshold of 1000 μm/m. According to Hammer [12], crack risk assessment from stress/strength is more reliable than using strain/strain capacity. If the tensile strength is lower than the stress level caused by restrained shrinkage, plastic shrinkage cracking occurs [12 13].

Many studies regarding the recycled concrete aggregates can be found in literature. These focus mostly on the effect of replacing natural aggregates by the recycled aggregates on long term prop erties (strength, creep and drying shrinkage) [17 19] while the studies related to the plastic shrinkage concern concrete with nat ural or lightweight aggregates. The plastic shrinkage is actually influenced by the initial water saturation of natural aggregates [20 21]. The effect of lightweight aggregate saturation on autoge nous shrinkage has already been investigated in literature [22]. The use of saturated lightweight aggregates is suggested to provide "internal" curing of the concrete. There is few published data on the influence of the recycled concrete on early age behaviour and plastic shrinkage.

The aim of the present experimental study is to quantify the cracking sensitivity of recycled concrete at early age, based on the monitoring of plastic shrinkage and mechanical properties. The experimental approach described in this paper is applied to concrete mixtures with different initial water saturation of recy cled aggregates and different rates of substitution of natural aggre gates by recycled gravel and sand. The water absorption and the saturation rates of the recycled aggregates used in this study were determined by combining experimental methods [23]. Plastic shrinkage measurements are associated with other experimental techniques to understand the evolution of plastic shrinkage and the influence of recycled aggregates. An approach based on direct tensile testing and calculated elastic stresses is then used to assess the cracking sensitivity. When the initial water saturation of recy cled aggregates varied, the added water content was adjusted to keep the total water content (W_{tot}) constant. The results obtained for all the concrete mixtures with different rate of saturation and substitution of recycled aggregates are presented, analyzed and discussed.

2. Materials and methods

2.1. Experimental program and mixtures

The experimental program focuses on two parameters. The first parameter of the study is the initial water saturation of coarse aggregates. The concrete mixture was made with 0% of recycled sand (RS) at saturated surface dry condition (SSD) and 100% of recycled gravel (RG) at different initial water saturations: 30%, 70%, 100% and 120% of SSD state. The second parameter is the substitution of natural aggregates with recycled aggregates, all (gravel and sand) being at the SSD state. Seven mixtures were designed in this study. Table 1 summarizes the details of the investigated concrete mixtures.

Two types of aggregates were chosen for this study: natural and recycled aggregates. Natural aggregates (NA) were crushed dark limestone aggregates. Recycled aggregates (RA) were obtained by crushing unknown waste concrete from the recycling plant of DLB Gonesse (Paris region, France). The RA used in this study are classified as aggregates type I, R_{CU95} [24] with R_{CU95}: 95% of products contained in a recycled aggregate are: concrete, concrete products, mortar, concrete masonry units, natural stone. These aggregates can be considered as good quality RA. Higher proportion of other materials, such as coatings or wood, would result in higher absorption thus lower strength of new concrete. Higher sulfate content due to gypsum could cause reactions with water and hydration products and possible damage in new cement paste. The water absorption coefficient (as % of dried mass after 24-h immersion) of each type of aggregate was defined according to the pycnometer and hydrostatic weighing [23]. The properties of aggregates used in the experimental study and the fines from sieve analysis are summed up in Table 2. The waste concrete source influences the content and properties of residual paste of RA [25]. The RA used in this study showed relatively fast absorption, which is typical of high W/C ratio of initial concrete and weak paste aggregate interface. Thus the residual paste volume is relatively low and this type of RA allows reaching adequate properties of hardened concrete. The packing density of each aggregate was determined experimentally according to the method LPC N°61 [26]. The determination of the specific surface was made according to the BET method, based on the adsorption of nitrogen gas on a surface. The amount of gas adsorbed at a given pressure allows the determination of the surface area [27]. The chemical analysis of the recycled aggregate is given in the Table 3.

Table 1
Details of the investigated concrete mixtures.

RS(%)-RG(%)	WS (%)			
	30	70	100	120
0–0			✓	
0–30			✓	
0–100	✓	✓	✓	✓
30–0			✓	

Note: RS: recycled sand, RG: recycled gravel, WS: water saturation.

Table 2
Properties of aggregates.

	Natural aggregates			Recycled aggregates			
	Sand 0/4 mm	Gravel 4/10 mm	Gravel 6,3/2 0mm	Fines <63 μm	Sand 0/4 mm	Gravel 4/10 mm	Gravel 10/20 mm
Mineralogy	Sandrancourt	Dark limestone	Dark limestone	Unknown waste concrete		Unknown waste concrete	Unknown waste concrete
Water absorption WA_{24} (%)	1.2	0.56	0.53	–	10.7	5.3	4.9
Density	2.6	2.73	2.73	–	2.1	2.34	2.32
Fines <63 μm (%)	0.6	0.4	0.3	–	2	0.9	0.7
Fines <125 μm (%)	3	–	–	–	7	–	–
BET (m^2/g)	1.03	–	–	9.9	5.3	–	–
Packing density of aggregates g*	0.693	0.588	0.586	–	0.755	0.580	0.561

Accepted Manuscript

Table 3
Chemical analysis of recycled aggregates [3].

	Recycled aggregates		
	Sand 0/4 mm	Gravel 4/10 mm	Gravel 10/20 mm
Total sulfur (%) EN 1744-1 (S)	0.20	0.13	0.30
Soluble sulfates in acid (%) EN 1744-1 (AS)	–	0.30	0.78
Soluble sulfates in water (%) EN 1744-1 (SS)	0.21	0.14	0.47
Soluble chlorides in water (%) EN 1744-1 (C)	0.0015	<0.0003	0.0004
Soluble chlorides in acid (%) EN 1744-5 (Ca)	0.02	<0.001	<0.001
Na_2O equivalent soluble (%) LPC 37 (Na_2O equi)	0.0305	0.0121	0.0151

Table 4
Properties of cement CEM II/A-L 42.5.

Chemical analysis (%)	
SiO_2	18.7
Al_2O_3	4.9
Fe_2O_3	3.7
CaO	62
MgO	1.3
SO_3	2.7
K_2O	0.68
Na_2O_3	0.17
S	0.05
Cl	0.04
CO_2	4.7
Free lime	1.5
Na_2O equivalent	0.59
Loss on ignition	5.1
Compound composition of clinker (%)	
C_3S	61
C_2S	–
C_3A	7.9
C_4AF	12
Physical properties	
Blaine finesse (cm^2/g)	3700
Normal compressive strength (MPa)	53
Density (kg/m^3)	3.09

The cement CEM II/A-L 42.5 (Table 4) from Rochefort (France) was made of clinker (87%), limestone (11%). Superplasticizer (SP) MC PowerFlow 3140 was also used. Table 5 summarizes the mixture proportions, the fresh concrete properties and the materials used in the seven mixtures. All the mixtures were established and optimized by the Compressive packing model (CPM) and the software BETONLAB [28]. The target slump referred to the workability class S4 [29]. The initial water saturation of sand was kept constant for all the mixtures at SSD value. The concrete designation 0RS-30RG-100SSD means that 0% (in mass) of recycled sand (i.e. there is only natural sand) and 30% (in mass) of gravel used is recycled, 100SSD means that the gravel it at SSD state. The Effective water to Equivalent Binder ratio is less than 0.65 ($W_{eff}/B_{eq} \leqslant 0.65$) for all the mixtures [30]. The Equivalent Binder content is determined according to European standard EN 206-1:

$$B_{eq} \quad Cement + k \times Limestone \tag{1}$$

k is the activity coefficient of limestone filler given by the standard ($k = 0.25$).

The water saturation of gravel is assessed from the gravel water content to water absorption in percent (W_{gravel}/WA_{24}). All the mixtures were designed keeping the total water (W_{tot}) constant [21] and the additional water (W_{added}) was calculated from the following equation:

$$W_{tot} \quad W_{added} + W_{aggregates} + W_{SP} \quad W_{eff} + W_{abs} \tag{2}$$

where: W_{tot}, water added in mixture containing dry aggregates; W_{added}, water actually added in the mixture; W_{eff}, the effective water content; W_{abs}, the water theoretically absorbed by dry aggregates; $W_{aggragates}$, the aggregates water content; W_{SP}, the water part of superplaticizer.

The packing density of aggregates (g^*) was calculated according to the procedure given by the software BETONLAB to allow the calculation of the maximum paste thickness (MPT) (Table 5). The MPT was given by the following equation:

$$MPT \quad D_{MAX}\left(\sqrt[3]{\frac{g^*}{g}} \quad 1\right) \tag{3}$$

with: D_{MAX}, Maximum size of aggregates; g^*: Packing density of aggregates; g, Aggregates volume.

Table 5
Properties and composition of concrete mixtures, with theoretical mixtures composed by dry aggregates and actual mixtures.

	0RS-0RG		0RS-30RG		30RS-0RG		0RS-100RG				
	100SSD		100SSD		100SSD			30SSD	70SSD	100SSD	120SSD
	Dry	Wet	Dry	Wet	Dry	Wet	Dry	Wet	Wet	Wet	Wet
NG 6,3/20 (kg/m^3)	820	824.3	462	464.4	829	833.4					
RG 10/20 (kg/m^3)			296	310.5			701	711.3	725.0	735.3	742.1
NG 4/10 (kg/m^3)	267	268.5	228	229.3	190	191.1					
RG 4/10 (kg/m^3)							163	165.6	169.0	171.6	173.4
NS 0/4 (kg/m^3)	780	789.4	813	822.8	549	555.6	806	815.7	815.7	815.7	815.7
RS 0/4 (kg/m^3)					235	260.0					
Cement, C (kg/m^3)	270		276		276		282				
Limestone, L (kg/m^3)	45		31		31		31				
Superplasticizer SP (kg/m^3)	0.747		0.861		0.798		0.798				
W_{eff} (kg/m^3)	180		185		185		189				
W_{tot} (kg/m^3)	194.6		212.3		221.4		241.0				
W_{SP} (kg/m^3)	0.6		0.7		0.6		0.6				
W_{sand} (kg/m^3)	0.0	9.4	0	9.8	0	31.6	0	9.7	9.7	9.7	9.7
W_{gravel} (kg/m^3)	0.0	5.8	0	18.2	0	5.5	0	12.9	30.0	42.9	51.5
$W_{absorbed}$ (kg/m^3)	15.2		28.0		37.1		52.6				
W_{added} (kg/m^3)	194.6	179.4	212.3	184.3	221.4	184.4	241.0	218.4	201.2	188.4	179.8
W_{eff}/B_{eq}	0.64		0.65		0.65		0.65				
Paste volume (L/m^3)	285		287		287		293				
Gravel/Sand	1.39		1.21		1.30		1.07				
Slump (mm)		195		193		204		222	215	195	193
Packing density of concrete g^*	0.785		0.781		0.790		0.777				
MPT (mm)	0.80		0.82		0.86		0.89				
Compressive strength											
$f_{c,\ 1d}$ (MPa)		6.4		5.8		4.2		4.3	4.6	4.1	5.4
$f_{c,\ 2d}$ (MPa)		10.3		11.7		10.0		7.8	8.9	9.5	9.6
$f_{c,\ 7d}$ (MPa)		23.0		22.1		19.4		12.2	19.9	18.7	–
$f_{c,\ 28d}$ (MPa)		31.4		28.5		29.0		24.0	26.6	27.6	28.8

Note: NG: natural gravel, NS: natural sand.

Accepted Manuscript

This parameter represents the mean distance between two coarse aggregates, assuming that each aggregate is surrounded by a paste layer [31]. The thickness is proportional to the aggregate diameter. The compressive strength has been found to decrease with an increase in the MPT [31]. In this study, the concrete mixtures have been designed to keep the MPT approximately constant (Table 5), in order to show the influence of the type of aggregates. The 30RS-0RG concrete mixture has slightly higher MPT because the packing density of recycled sand (Table 2), and thus the packing density of concrete, is higher than the packing density of natural sand. The MPT of 0RS-100RG is higher than 0RS-0RG because its paste volume is slightly higher (Table 5).

2.2. Testing procedures

2.2.1. Plastic shrinkage

The tests were performed in an air-conditioned room with a temperature of 20 ± 1 °C and relative humidity (RH) of 50 ± 5% and started about 30–40 min after the first contact between water and cement. The plastic shrinkage development was measured using two identical steel moulds ($70 \times 70 \times 280$)mm^3 covered on the inside by Teflon, limiting friction between concrete and the mould [32]. The concrete was cast in a plastic sheet between two PVC plates. Their displacement is measured without contact by two laser sensors. Both ends of the steel mould are drilled in the center. The circular opening allows monitoring the movement of the reflecting plates anchored to the edges of the specimen (Fig. 1). The temperature of concrete sample was kept at 20 °C by water circulating along the sides and the bottom of the steel mould. The uncertainty on the plastic deformation was ±50 μm/m.

Several properties were monitored in parallel of plastic shrinkage to understand the evolution of plastic shrinkage: weight loss, setting time, capillary pressure, and evolution of elastic properties at early age, and hydration using an isothermal calorimeter. All data were logged on a computer every 10 min during a period of 24 h.

2.2.2. Weight loss

The water loss was monitored for all the mixtures using a data recording scale. The concrete was poured in cylindrical moulds $\text{Ø}11 \times 7$ cm^2 in order to have the same environmental conditions as the plastic shrinkage measurement. Only the upper surface was subjected to drying conditions. From mass loss, the rate of evaporation in kg/m^2 was determined by dividing water loss by the surface of the cylinder.

2.2.3. Capillary pressure

The main driving force of plastic shrinkage is the capillary pressure. In dry and/or hot weather the water covering the surface may evaporate. If this takes place, a complicated system of menisci is formed by the water between the particles near the surface of concrete (due to desiccation) or inside the material (due to self-desiccation) [33–35]. The capillary pressure was measured by the test setup described in (Fig. 2), using a porous ceramic cup placed horizontally in the middle of a cylinder [36]. The mould has the same depth and drying conditions as the specimens used to measure the mass loss and the plastic shrinkage. The ceramic cup was connected to a pressure sensor using a thin tube. The uncertainty on the capillary pressure was ±2% of the average value.

2.2.4. Setting time

According to the European standard EN 196-3 [37], the Vicat test was used to monitor initial and final setting time for all the mixtures. The concrete was poured in a 5 mm sieve to obtain mortars for the test. The samples were placed in temperature controlled water (at 20 °C) to prevent mortar from drying. The setting time is indicated by rapidly increasing penetration resistance. The monitoring of the setting time was done by using an automatic device. The uncertainty on the setting time was ±0.5 h.

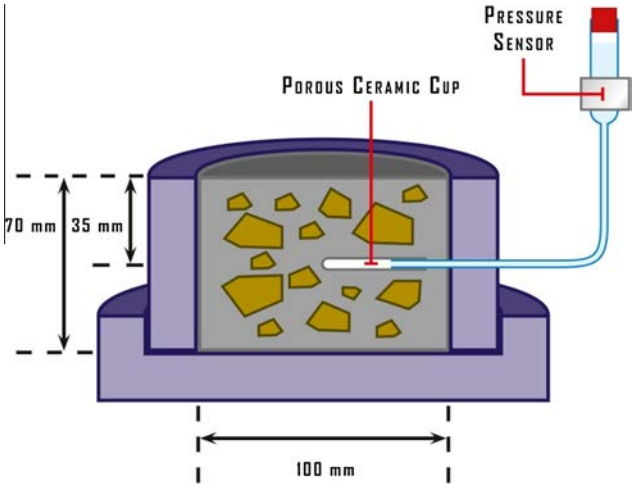

Fig. 2. Schematic section of capillary pressure device.

2.2.5. Elastic properties of concrete at early age

The evolution of elastic properties of concrete at early age was monitored by the *FreshCon* system which measures the velocity of ultrasonic pressure (*p*) and shear (*s*) waves [38] (Fig. 3). This device was originally developed at the University of Stuttgart to analyze the setting and hardening of any kind of material (especially fresh cement paste and fresh mortar). The testing device consists of a mould constituted of two polymethacrylate (PMMA) walls and held by four screws. It is equipped with an ultrasonic emitter and transducer (transmitter and receiver). The U-shaped mould is made of foam with high damping properties to absorb the waves through the mould and travelling around the concrete specimen (concrete volume of 450 cm^3). A pulse signal is generated (800 V with a pulse width of 2.5 μs) at selected regular intervals during this test and the amplitude is enhanced by an amplifier. The ultrasonic longitudinal compression waves are then transmitted through the concrete sample and then the signal is received by an ultrasonic receiver after travelling through the sample and sent back to the data acquisition card (DAQ card). The software automatically calculates the time it takes for the wave to travel from the transmitter to the receiver and deduces the velocity. The uncertainty on the velocity was ±5% of the average value. The concrete sample was protected by a plastic sheet to avoid drying and the temperature was measured in the middle of the specimen using a thermocouple. The test was performed in an air-conditioned-room at 20 °C and 50% RH. The evolution of dynamic properties (Poisson's ratio υ_{dyn}, shear modulus G_{dyn} and elastic modulus E_{dyn} in MPa) was obtained as a function of the velocity of the compression waves and the shear waves using the following equations:

$$\upsilon_{dyn} \quad \frac{\frac{1}{2}v_p^2 \quad v_s^2}{v_p^2 \quad v_s^2} \tag{4}$$

$$E_{dyn} \quad v_p^2 \cdot \rho_c \cdot \frac{(1+\upsilon_{dyn}) \cdot (1 \quad 2\upsilon_{dyn})}{1 \quad \upsilon_{dyn}} \tag{5}$$

$$G_{dyn} \quad v_s^2 \times \rho_{concrete} \tag{6}$$

Where ρ_c is the density (kg/m^3), V_p is the P-wave velocity (m/s) and Vs the S-wave velocity (m/s).

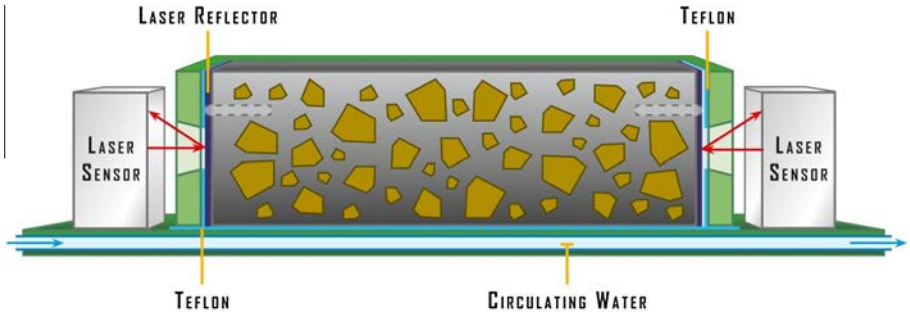

Fig. 1. Plastic shrinkage testing device with temperature control.

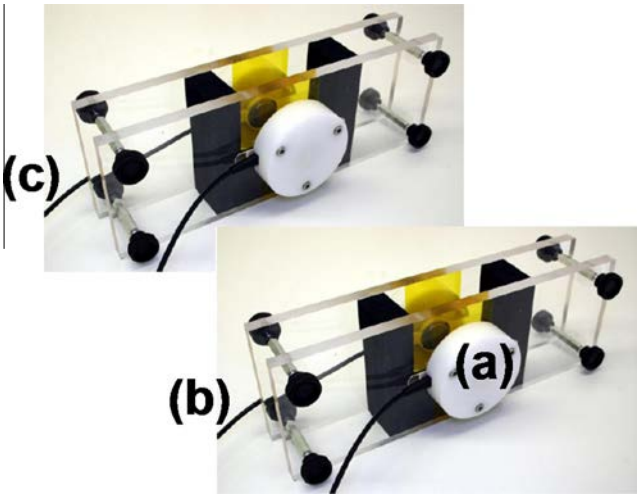

Fig. 3. Test container for ultrasonic monitoring device, (a) Piezoelectric sensor, (b) P-wave mould, (c) S-wave mould.

2.2.6. Tensile strength

Tensile strength of concrete was determined from direct tensile tests. The device (Figs. 4 and 5) and the experimental procedure were designed to study the early-age behaviour of concrete [9]. The load is applied horizontally by an electric displacement-controlled actuator. The load cell is placed between the actuator and the mobile part of the mould. The dogbone shaped mould actually comprises two halves with curved transitions to a central part with reduced constant section, 100 mm high, 100 mm long, and 105 mm wide. The inner face of the mould is covered with PTFE and protected with thin polyethylene sheets during the test. The two parts of the mould are linked to the frame and the load cell by spherical pin connections. The stress was deduced from the measured load and the cross section (100×105 mm^2). The concrete specimen was cast in the steel mould just after mixing then vibrated in one layer. An external frame was placed on the plate to avoid displacements of the two halves of the mould due to the vibration and pressure of fresh concrete. The specimen was covered until testing with a polyethylene sheet to avoid drying. The ambient temperature was 20 °C. The loading rate of the actuator was 5 μm per second. The tests have been done twice for each concrete mixture. The average difference between two strength values at the same age was 6%.

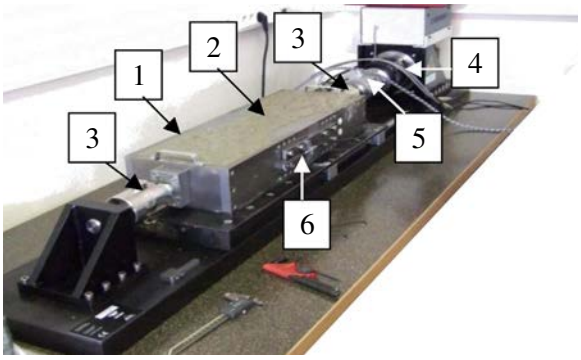

Fig. 4. Direct tensile testing machine: 1: Steel mould, 2: Concrete specimen, 3: Spherical pin connection, 4: Electric actuator, 5: Load cell, 6: LVDT2.

2.2.7. Isothermal calorimetry

An isothermal calorimeter TAM air was used to measure the heat flow of concrete, in order to understand better the influence of hydration on the properties of concrete at early age. It is designed for sensitive and stable heat flow measurement with an operating temperature range between 5 °C and 90 °C. In this study, a temperature of 20 °C was used for all the concrete mixtures to have the same conditions as the other tests. The isothermal calorimeter contains three separate channels; all calorimetric channels are of the twin type, consisting of sample and reference chamber. A polished glass ampoule with a 125 ml volume was used. The sensitivity of the heat detectors is in the μW–mW range. The thermostat stability is ±0.02 °C, the limit of detection 4 μW, and the precision ±20 μW.

The principle of the calorimetric measurement derives from to the general heat balance equation (Eq. (7)). The details of a calorimetric unit are shown in (Fig. 6). When a sample is placed in the unit, the heat produced by hydration will flow rapidly to its surroundings. The main route for heat exchange between the sample and the surroundings is through the heat flow detector, consisting of small plates with thermopiles. The heat flow, caused by the temperature difference across the sensor, creates a voltage signal proportional to the heat flow. This voltage signal is corrected by the reference and converted to the rate of heat evolution by applying the calibration factor. After calibration, the rate of heat production (dQ/dt) is equal to the heat flow monitored by TAM air.

$$\frac{dQ}{dt} \quad \Phi + c \cdot \left(\frac{dT}{dt}\right) \tag{7}$$

where (dQ/dt) is the rate of heat production (J·s ^{1}), Φ the rate of heat exchange (the measured property (J·s ^{1})), C heat capacity (J/°) and $C(dT/dt)$ the rate of heat accumulation (J·s ^{1}).

In order to control the test condition, the isothermal calorimeter was placed in a temperature- controlled-room at 20 °C and the test was started 30 min after adding water in the mixer.

3. Experimental results and discussion

3.1. Analysis of early age behaviour and correlations

The results of plastic shrinkage showed a good repeatability, as the maximum difference between the total deformations of two samples was lower than 5% (Fig. 7). Other monitored properties (early age hydration, setting time, capillary pressure, weight loss

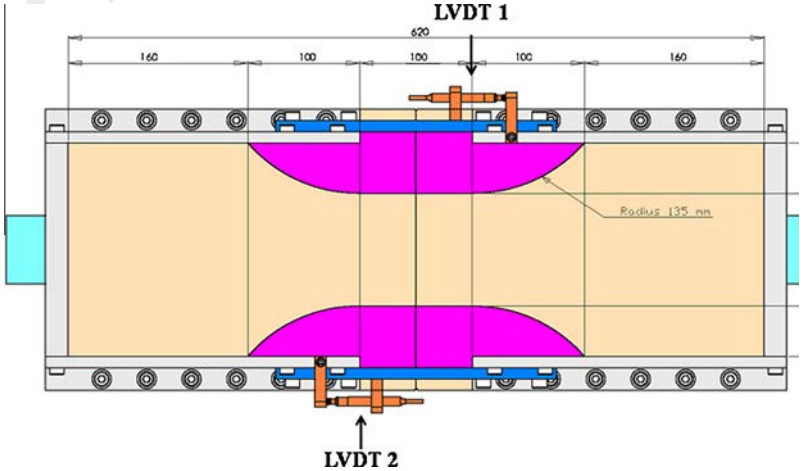

Fig. 5. Mould used for direct tensile tests.

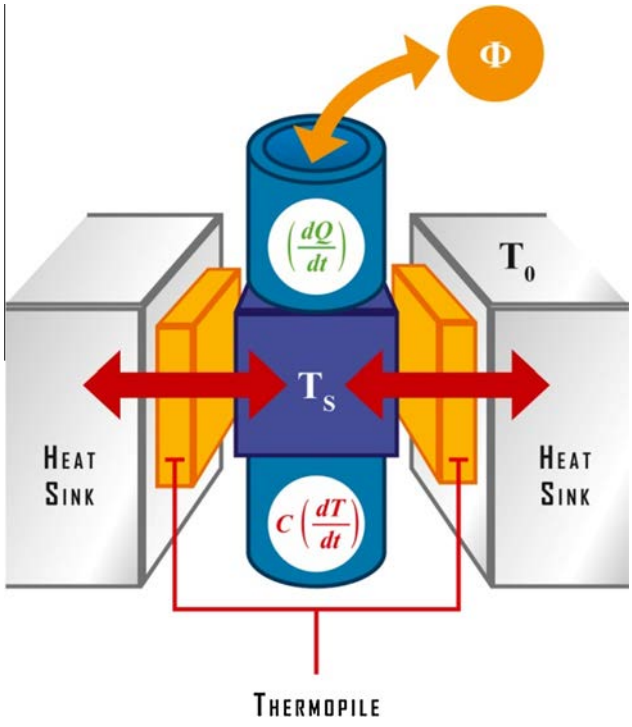

Fig. 6. Isothermal calorimeter TAM air (calorimetric unit [39]).

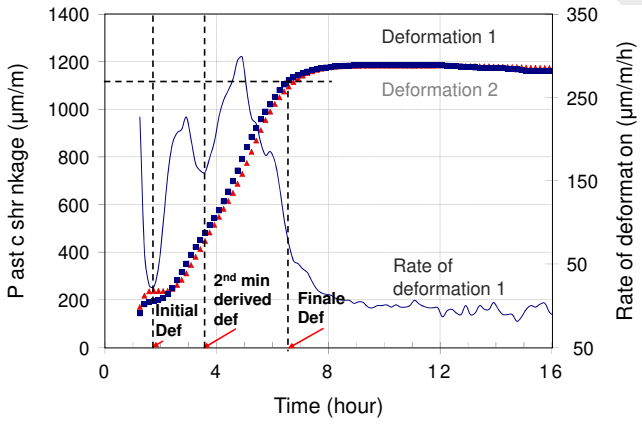

Fig. 7. Deformation evolution and its derivative, concrete 0R-100R-70SSS.

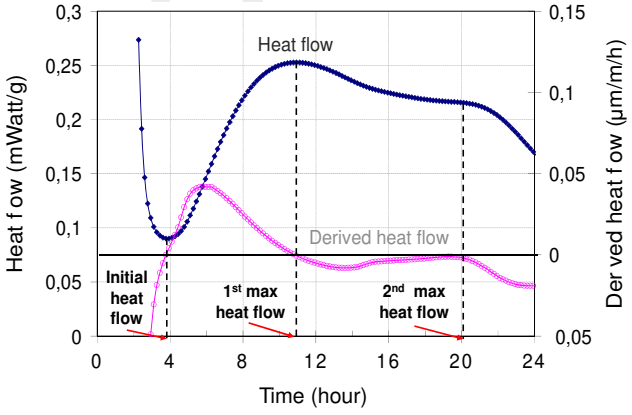

Fig. 8. Heat flow evolution and its derivative, concrete 0R-100R-70SSS.

and evolution of elastic properties) are shown in (Figs. 8 11 and 14) respectively, to understand the phenomena occurring during the plastic shrinkage development. The curves presented in (Figs. 7 11 and 14) relates to concrete 0RS 100RG 70SSS. For each curve, several interesting time points were defined. The same data processing was made for all concrete presented in Table 1. The cor relations between these points are shown on Figs. 12 and 13.

The derivative of the deformation actually gives two minima (Fig. 7). The first minimum generally occurs during the first two hours. Before this point, the plastic shrinkage rate is high and decli nes rapidly. It corresponds to the thermal deformation, as the tem perature of fresh concrete after mixing is different from the temperature in the plastic shrinkage moulds (20 °C). All the follow

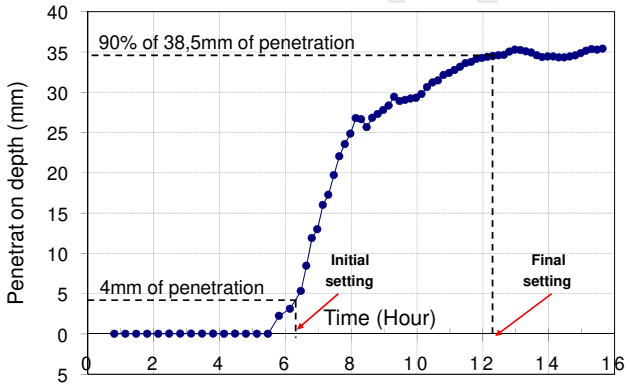

Fig. 9. Initial and final setting time, concrete 0R-100R-70SSS.

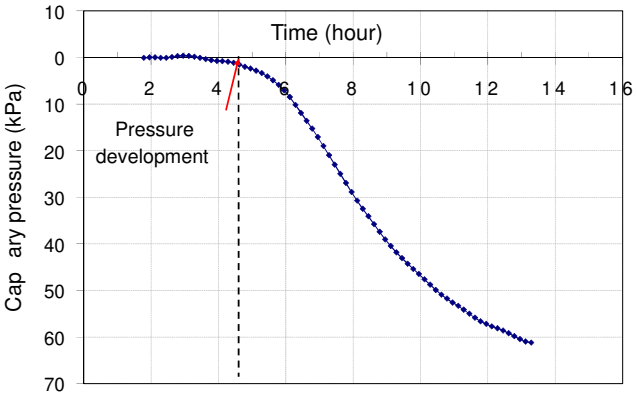

Fig. 10. Capillary pressure development vs. time, concrete 0R-100R-70SSS.

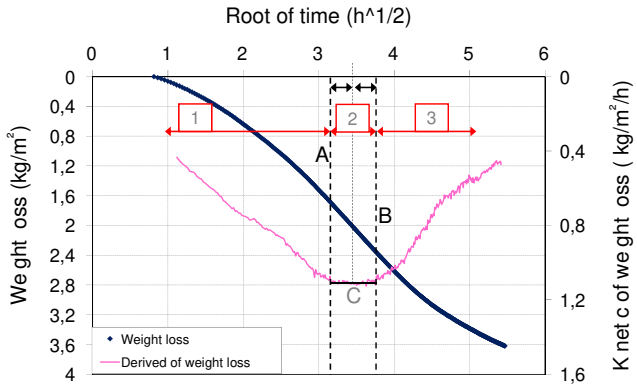

Fig. 11. Weight loss vs. Square root of time, concrete 0RS-100RG-70SSS.

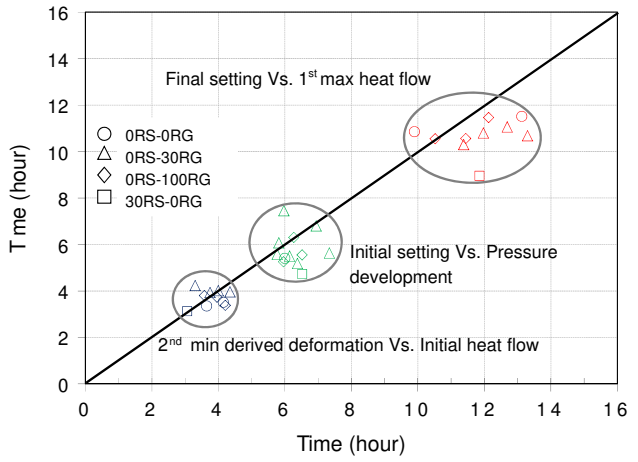

Fig. 12. Correlation between different parameters, concrete summarized in Table 1.

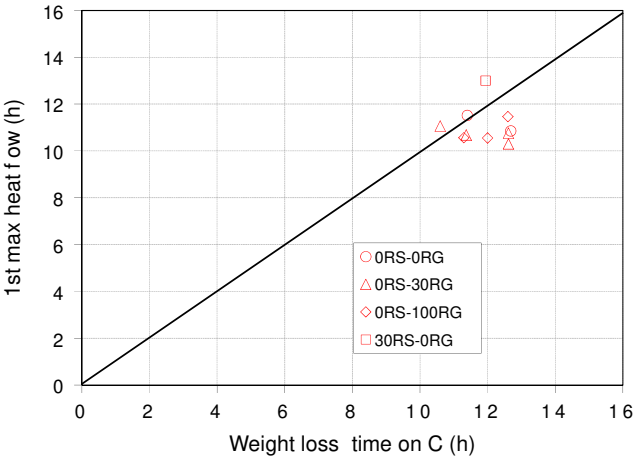

Fig. 13. Correlation between time in C and 1st max of heat flow, concrete summarized in Table 1.

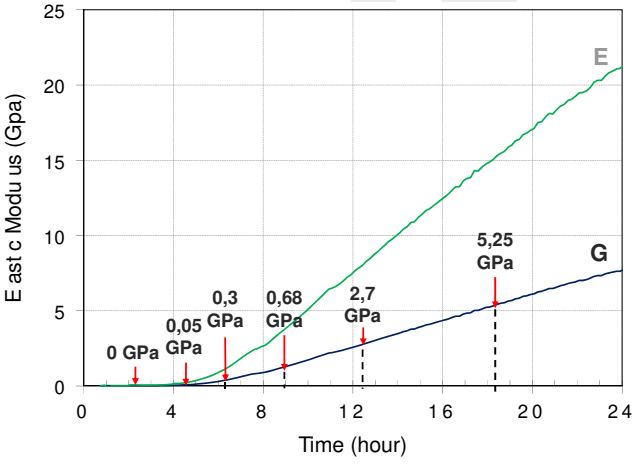

Fig. 14. Evolution of elastic properties at early age, concrete 0RS-100RG-70SSS.

ing curves of plastic shrinkage are initialized at the first minimum of derived deformation, noted (Initial def). It has no consequence of stress development as the Young modulus is still relatively low (Fig. 14). The second point is noted as (2nd min derived def). The third point corresponds to 95% of the maximum deformation. Between (Initial def) and (2nd min derived def) the rate of plastic shrinkage increases then decreases until a minimum. At the end of this stage, initial setting has not occurred, the capillary pressure has not diminished, and the elastic modulus is still relatively low. Thus shrinkage observed during this stage is likely to be caused by chemical shrinkage of cement paste.

The hydration process is also characterized by several stages [40]. To describe these stages, the derivative of heat flow was drawn. Three times, corresponding to the points where this deriva tive equals zero, were defined as initial heat flow, 1st max heat flow and 2nd max heat flow (Fig. 8). The initial heat flow corre sponds to the dormant period and concurs quite well with the time of (2nd min derived def). Also, the period before 1st max heat flow is related to the acceleration period and this time has a good cor relation with time of final setting (Fig. 9). The result is presented in Fig. 12. The characteristic time corresponding to (2nd min derived def) coincided well with the point corresponding to the start of the heat flow (Fig. 8). These two points showed good cor relation (Fig. 12). The acceleration phase of the plastic shrinkage is controlled by the onset of hydration.

Then Initial setting occurs (Fig. 9), which corresponds to the beginning of capillary pressure development (Fig. 10). At this time the value of shear modulus was 0.3 GPa. As long as cement paste remains fluid, autogenous deformation is equal to chemical shrink age. Then, as the stiffness of the paste increases, the hydration of cement causes cavitations and the creation of voids in the cement matrix. The time characterized by capillary pressure development (Pressure development), shown in Fig. 10, matches the appearance of menisci in the pores and between the cement matrix and the ceramic porous sensor [33 35]. Capillary pores were initially filled with water. As water is consumed by the hydration of cement, voids appear and liquid vapour menisci are created in the pores. The maximum plastic shrinkage rate was observed between (2nd min derived def) and time noted (Final def). During this stage cap illary pressure significantly decreases. Shrinkage is actually caused by capillary depression, by self desiccation shrinkage and external drying. But in the same time elastic and shear modulus signifi cantly progress, which finally prevents concrete from shrinking.

The exploitation of data of weight loss at the early age can be considered as an analytical tool to explain phenomena due to dry ing. In order to perform this, the weight loss and it derivative was plotted as function of the square root of time. Three stages can be distinguished (Fig. 11). The first stage is characterized by a high drying rate due to the water lost from surface (bleeding water). During the same stage the decrease of drying rate was observed around 5 h; it could correspond to the drying of concrete with cre ation of menisci that generates capillary depression (see Fig. 10) and accelerates shrinkage. During the second stage a constant dry ing rate was observed (with the square root of time scale). The final stage was characterized by a decrease of the rate and finally a sta bilization of the weight loss curve.

The characteristic time defined as the point C (time from the middle of the 2nd phase) correlates well with the time correspond ing to the 1st maximum heat flow. The plastic deformation evolu tion is actually caused by hydration and drying. As hydration accelerates, capillary pores are created and begin to empty because of drying, thus the drying rate change. This behaviour was the same for all the mixtures (Fig. 11). Moreover, the time in point C can be associated with the final setting.

For all the mixtures, the shear modulus G starts to develop when the first hydration products are formed, filling up the pore space and creating a denser structure. Thus, an increase in shear modulus will cause a growth in the S wave velocity but not in pen etration resistance (G = 0.05 GPa). During the first hours, when the cement particles are connected, the shear modulus and thus the penetration resistance start to develop [41]. This time corresponds

to pressure development and the initial setting (G = 0.33 GPa). For most mixtures, the final setting determined with Vicat test relates quite well with the time of 1st max heat flow and it corresponds to G = 2.7 GPa.

Therefore, from all the time points defined previously, a time line was established to understand early age parameters development (Fig. 15). In addition, the thresholds G = 0.33 GPa and 2.7 GPa are proposed to easily determine initial and final setting respectively based on the ultrasonic measurements.

3.2. Effect of the water saturation of recycled aggregates

The plastic shrinkage measurements on the concrete 0RS 100RG with different initial water saturation of gravel showed minor differences. The magnitude at 24 h was between 870 and 1055 µm/m (Fig. 16a). The value of 1000 µm/m at 24 h has been proposed in the literature [15] to characterize high risk of cracking of concrete at early age. Only one concrete mixture (100SSD) showed a 24 h shrinkage higher than this critical value.

The mixture with saturated gravel (100SSD) actually showed the highest plastic shrinkage and those with gravel at 30% initial saturation and oversaturated (30SSD and 120SSD respectively) showed the lowest values. The influence of added water content was confirmed by the variations of compressive strength at 28 days (Table 5). The extra water content which is theoretically absorbed by partially saturated aggregates was actually not fully absorbed, resulting in higher effective water than the theoretical effective water content. The concrete with 30SSD has the higher added water (W_{added} = 218.4 kg/m^3, $W_{aggregates}$ = 22.6 kg/m^3), which implies a higher bleeding rate [42]. As a result, the bleeding rate played an important part in minimizing the plastic shrinkage of concrete at 30SSD state. The concrete with oversaturated gravel (120SSD) has a low shrinkage as well. This mixture was characterized by the same total water as concrete 30SSD (W_{added} = 179.8 kg/m^3, $W_{aggregates}$ = 61.2 kg/m^3). Oversaturated gravel actually releases water in cement paste and provides self curing in concrete [22].

Absorption measurements on different aggregates showed a relatively high water saturation rate of recycled aggregates during the first hour [23]. After two hours, the water saturation actually reached 90% (Fig. 16b). Therefore, when the development of plastic deformation begins, the major part of water saturation has already occurred, which explains that the weak effect of initial water saturation.

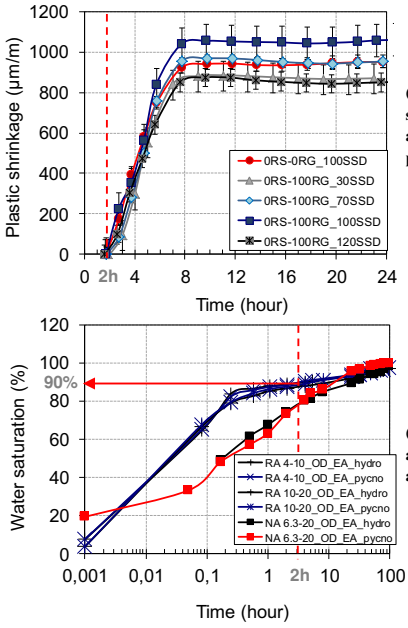

(a) effect of water saturation of recycled aggregates concrete on plastic shrinkage.

(b) Influence of aggregate type on water absorption rate [23].

Fig. 16. Correlation between plastic shrinkage and rate of water absorption.

3.3. Effect of the recycled aggregates substitution

The measurement of plastic shrinkage began 30 60 min after cement water contact. In this study, all the curves were initialized at the age of Initial def defined previously (Fig. 7). The graphs (Fig. 17) showed the influence of the percentage of substitution of recycled aggregate (gravel or sand) on plastic deformation. A higher deformation was observed when the recycled sand was used compared to conventional concrete with a difference of 47% after a period of 8 h.

The most significant plastic shrinkage concerned concrete with recycled sand (Fig. 17). Recycled sand had the highest coefficient of absorption and percentage of fines. The recycled sand and fines with a size lower than 63 µm develop a surface area of 5.3 m^2/g and 9.9 m^2/g respectively (Table 2). As a consequence, the effective water intended for the cement paste is attracted and kept in the menisci created by the recycled fines. Therefore, the bleeding water is lower than in the control mix and the risk of plastic shrinkage related to insufficient curing increases.

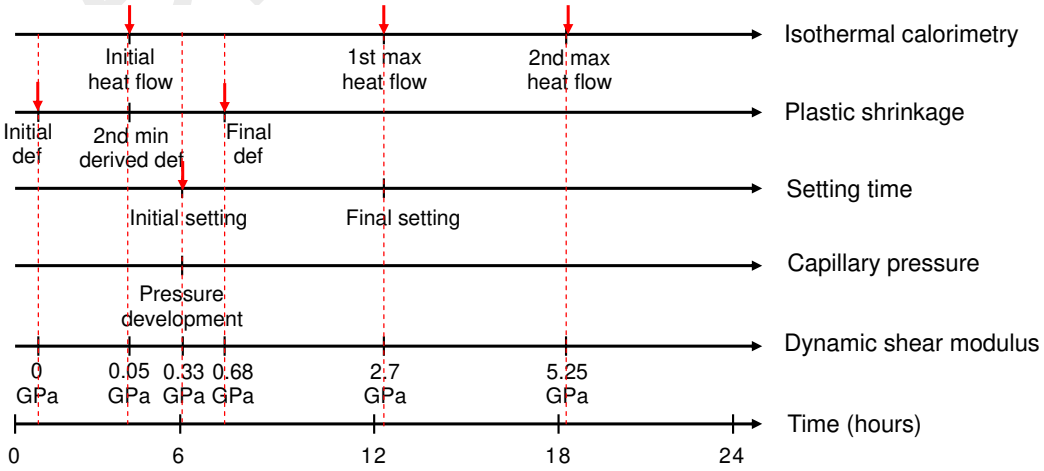

Fig. 15. Schematic timeline of early age parameters.

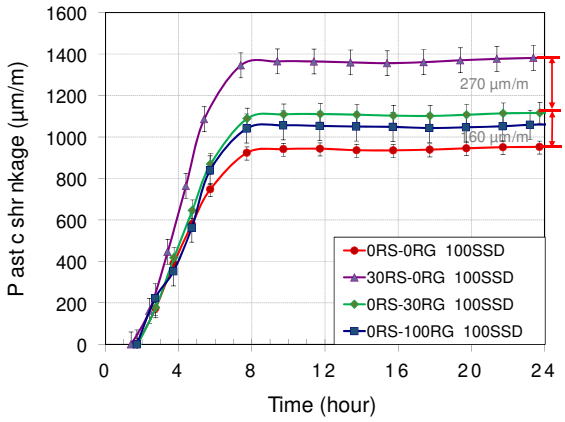

Fig. 17. Effect of substitution rate on plastic shrinkage.

The plastic shrinkage in recycled concretes with substitutions of 30% and 100% of recycled gravel were close. When they are com pared with the concrete 0RS 0SG_100SSD (red curve), the differ ence is significant but lower than 10%. The values of Maximal Paste Thickness (MPT) of the three concrete mixtures were actually very close. The MPT corresponds to the distance between two coarse aggregates. It is the distance between two particles, in a uni form dilation process corresponding to the injection of cement paste in the aggregates mix [31,43]. By using the software BETON LAB [28], the MPT was calculated for the four mixtures and the results found show a quasi constant MPT (Fig. 18), knowing that the shrinkage of concrete mainly comes from free shrinkage of cement paste in MPT. The recycled concrete 0RS 100RG_100SSD has a higher value of MPT (0.89 mm) than 0RS 30RG_100SSD (0.82 mm) but it showed lower plastic shrinkage. Several phenom ena could explain this variation. The 0RS 30RG concrete mixture had lower total water content (Table 5), thus lower potential self curing provided by porous recycled aggregates. However, the restraining effect can be expected to be lower when recycled aggregates are used in substitution of natural aggregates, thus the shrinkage of 0RS 100RG concrete should be higher. Recycled aggregates are made of residual cement paste and initial natural aggregates. Cement paste generally shows lower elastic modulus than natural aggregates and the crushing process is likely to induce micro cracks in residual paste, thus recycled aggregates show lower elastic modulus than natural aggregates. The elastic modu lus of aggregates used in this study was determined by the authors [44]. The values of recycled aggregates were lower compared to the natural aggregates ($E_{recycled\ sand}$ = 24.6 GPa, $E_{natural\ sand}$ = 42.3 GPa, $E_{recycled\ gravel}$ = 54.2 GPa and $E_{natural\ gravel}$ = 78.3 GPa). Finally, in spite of higher MPT and lower restraining effect

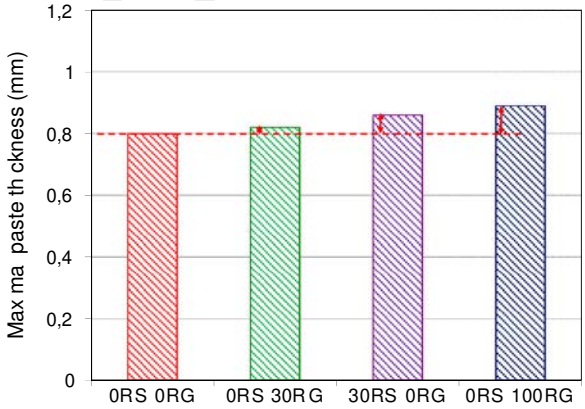

Fig. 18. Effect of substitution rate on MPT.

of recycled aggregates, 0RS 100RG concrete showed lower plastic shrinkage than 0RS 30RG concrete. This result suggests that inter nal curing provided by initially saturated recycled aggregates cur ing had a significant effect on shrinkage.

The experimental result of the study allows investigating the correlation between the hydration degree and the modulus E_{dyn}. The degree of hydration $\alpha(t)$ is often estimated by using experi mental methods based on the exothermic character of the hydra tion process:

$$\alpha(t) \quad Q(t)/Q_{max} \tag{8}$$

where $Q(t)$ is the cumulated heat developed at a time t, in J/g and Q_{max} is the maximum total heat corresponding to complete hydra tion, in J/g. Q_{max} is determined by extrapolating the heat flow vs. $1/\sqrt{t}$ curves. The cumulated heat Q(t) can be calculated as follows:

$$Q(t) \quad \int_0^t q(t) \cdot dt \tag{9}$$

where $q(t)$ represents the heat flow assessed by isothermal calorimetry, expressed in mW/g/s.

The analytical model of Eurocode 2 based on a function of time is not adapted to assess the mechanical properties of early age concrete when comparing the predicted and experimental values [45]. The reason is probably related to the model parameters. Therefore, several researchers [45 47] have proposed models based on the hydration degree in order to predict the evolution of the mechanical properties. The development of hydration strongly affects the evolution of the Young modulus. The Eq. (9) is used in this study to model the evolution of dynamic Young modulus as a function of the hydration degree. The modulus E_{dyn} was measured by using non destructive methods: *FreshCon* system between 0 and 48 h then dynamic method based on natural fre quencies between 2 and 28 days. The parameter E_{28d} is determined from the experimental results, the coefficients a and b are fitted from experimental data (Table 6).

$$E_{dyn}(\alpha) \quad a \times E_{28d}(1 \quad \exp^{\,b\times\alpha(t)}) \tag{10}$$

Table 6
Parameters of Eq (10) for the four mixtures.

	E_{28d} (GPa)	a	b
0RS-0RG_100SSD	39	1.44	1.33
30RS-0RG_100SSD	35.6	1.50	1.34
0RS-30RG_100SSD	38.7	1.10	2.84
0RS-100RG_100SSD	34	1.33	1.62

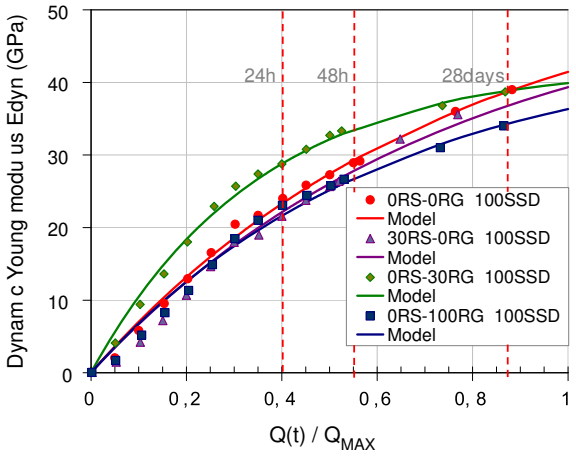

Fig. 19. Young's modulus vs. hydration degree.

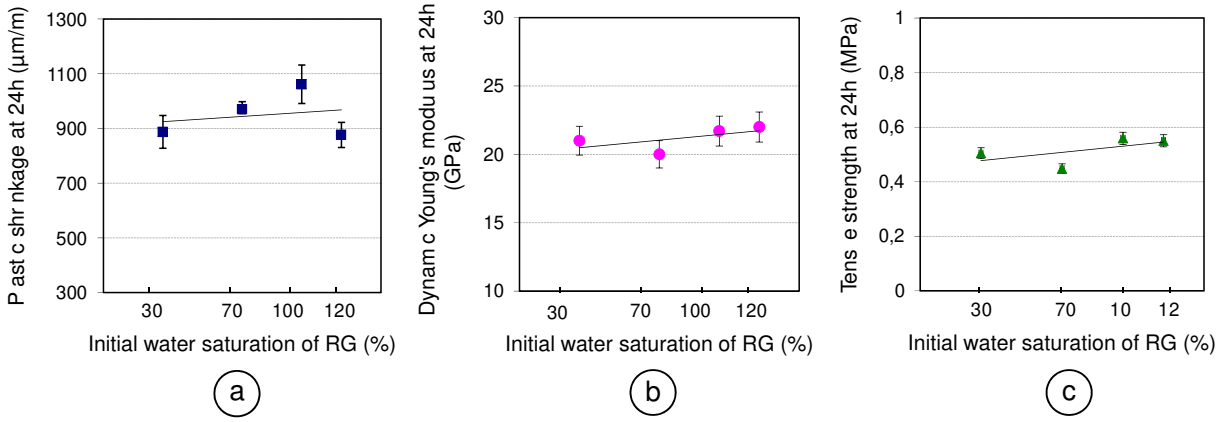

Fig. 20. Influence of initial water saturation of RG on early age properties.

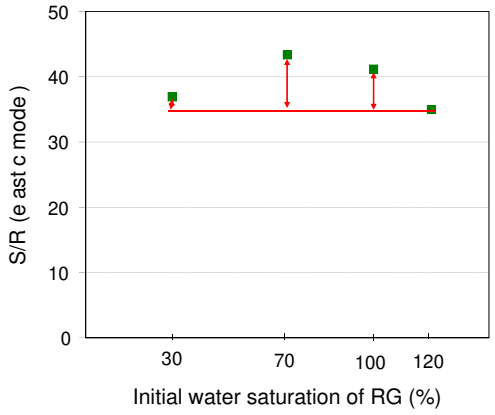

Fig. 21. Influence of initial water saturation of RG on cracking sensitivity.

A good correlation between this model and experimental data was found, as shown in Fig. 19. The four concrete mixtures showed a similar behaviour at early age (0 24 h) with the exception of the concrete with 30% of RG. The concrete 0RS 30RG_100SSD did actu ally not show an intermediate behaviour between the concrete mixtures with 0% and 100% recycled gravel. At the same hydration degree, the concrete 0RS 30RG developed a higher modulus at early age. This concrete also showed higher magnitude of plastic shrinkage than expected from the magnitudes of 0RS 0RG and 0RS 100RG. 0RS 30RG concrete also showed relatively high value of E_{28d} (Table 6). The substitution of 30% recycled sand and 100% recycled gravel resulted in lower elastic modulus at 28 days, but the evolution at early age were similar to conventional concrete, thus mainly governed by cement paste. Additional tests would be necessary to generalize the Eq. (10) for concretes with different rates of substitution and Effective water/Cement ratios.

3.4. Early age cracking risk of recycled concrete

In the present experimental study, the objective is to compare the shrinkage induced cracking sensitivity of different conven tional and recycled concretes at early age, based on monitoring of the evolution of stress and strength. Previous works actually showed that failure occurs when the restraining stress exceeds the tensile strength [12], [13]. Plastic shrinkage is likely to generate such restraining stress. The evolution of plastic shrinkage and ten sile strength has been experimentally assessed using specific tests [9]. However, an elastic uncoupled approach was used to assess the evolution of stresses due to restrained shrinkage (Eq. (11)):

$$\sigma(t) \quad \varepsilon(t) \times E(t) \tag{11}$$

where: $\varepsilon(t)$ is plastic shrinkage deformation, $E(t)$ is Young modulus evolution and $\sigma(t)$ is the estimated stress produced by total restraint. The value of $\sigma(t)$ at 24 h is noted S.

The concrete tensile strength, noted R, was experimentally assessed 24 h after casting using direct tensile test. The experimen tal approach is first applied to the reference concrete and concrete mixtures with different rates of saturation by keeping sand at sat urated state then different rates of substitution (recycled gravel

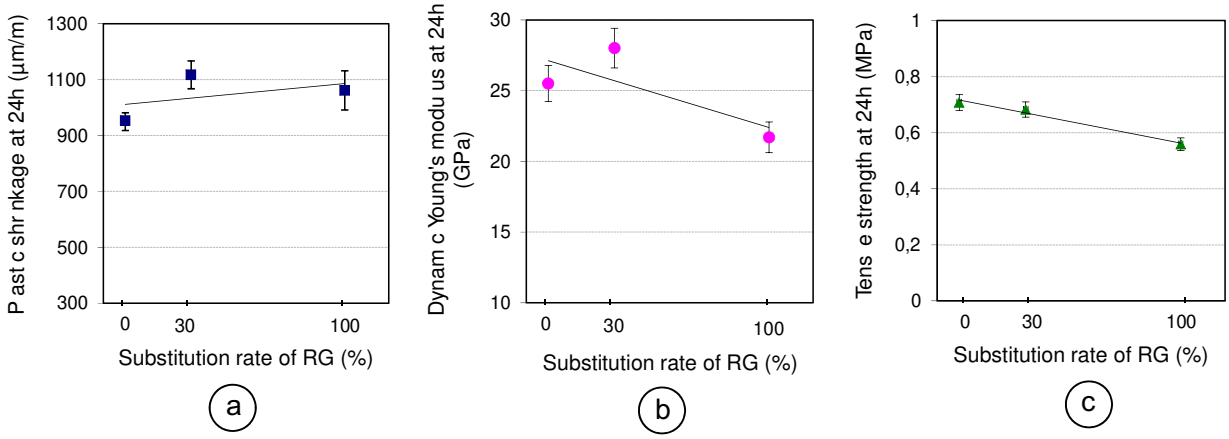

Fig. 22. Influence of substitution rate of RG on early age properties.

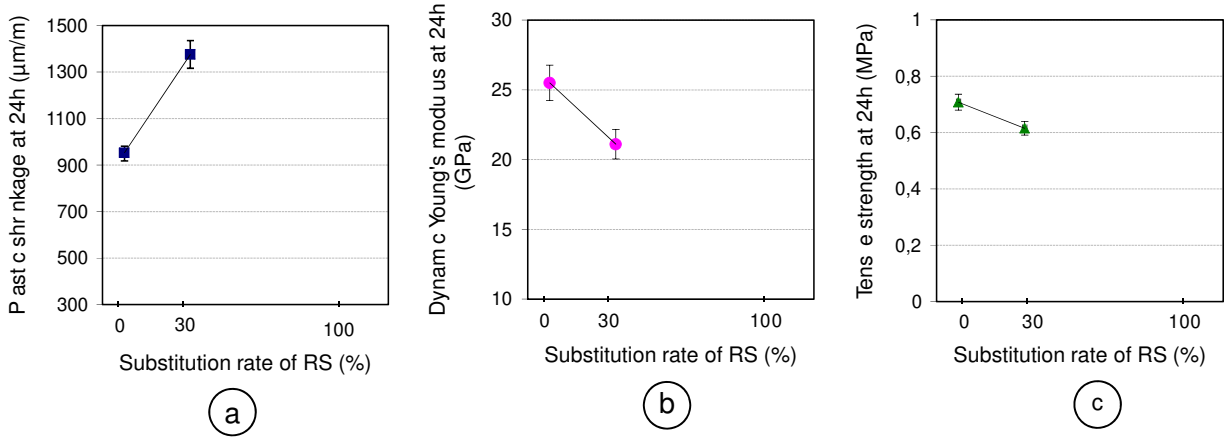

Fig. 23. Influence of substitution rate of RS on early age properties.

and recycled sand). Saturated sand was used is all mixtures. Thus, the study aims at quantifying the cracking sensitivity of recycled concrete at early age, based on comparing the *S*/*R* ratio of the dif ferent mixtures. The cracking sensitivity is assumed to increase with the S/R ratio.

The values of plastic shrinkage and mechanical properties (elas tic modulus and tensile strength) at 24 h show that the effect of initial water saturation of RG was negligible (Fig. 20).

Nevertheless, the *S*/*R* ratio of the concretes 70SSD and 100SSD is higher than concrete 30SSD (Fig. 21), thus, their cracking sensitiv ity is relatively high. This behaviour is confirmed in other study [21]. The plastic shrinkage magnitude of concrete 100 SSD actually exceeded the threshold of 1000 µm/m [14 16]. The effects of relaxation are not taken into account in this analysis. However the four concrete mixtures with different initial water saturation of aggregates can be expected to show the same relaxation, as they have the same paste volume and W_{eff}/B_{eq} ratio. In literature, creep is reported to increase with Water/Beq ratio [48]. The increasing of water added/B_{eq} ratio is accompanied by a decrease in compressive strength (Table 5) which implies an increase of the creep deforma tion according to the Eurocode 2 model [49]. As a consequence, the concrete 30SSD would have the highest benefit from relaxation and the lowest cracking sensitivity, as it has the highest Water added/B_{eq} ratio.

The percentage of substitution of recycled gravel or sand signif icantly affected the plastic shrinkage magnitude and the mechani cal properties, such as elastic modulus and tensile strength, and early age deformation (Figs. 22 and 23), resulting in a higher crack ing sensitivity of concrete mixtures with recycled aggregates. The concrete 0RS 30RG and 30RS 0RG are characterized by a higher stress development due of the fast growth of elastic modulus (Fig. 22b) and plastic deformation (Fig. 23a) respectively which implies higher *S*/*R* ratios.

Consequently, the sensitivity of both concretes is higher than the other concretes with 0% or 100% recycled gravel (Figs. 24 and 25). The effect of relaxation is not taken into account here. Creep or relaxation phenomena take place en cement paste. Thus increas ing paste volume results in higher relaxation. The concrete mix tures of the study were designed keeping the paste volume and the MPT approximately constant. However recycled aggregates are made of natural aggregates and old paste. As a consequence concrete with recycled aggregates can be expected to show higher relaxation, thus lower actual stresses. The proportion of recycled gravel (and consequently old paste) in 0RS 30RG concrete is rela tively low, whereas it is significant in 0RS 100RG concrete. Finally, in this study, concrete with 100% recycled gravel is likely to show lower cracking sensitivity than concrete with 30% recycled gravel.

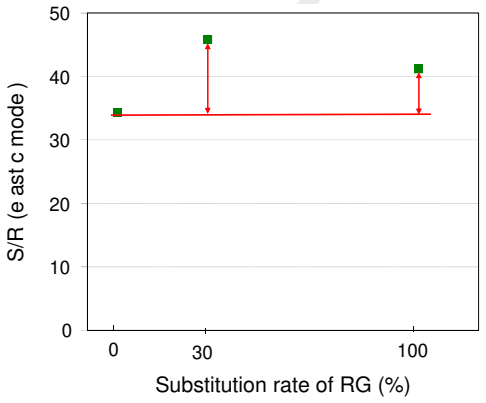

Fig. 24. Influence of substitution rate of RG on cracking sensitivity.

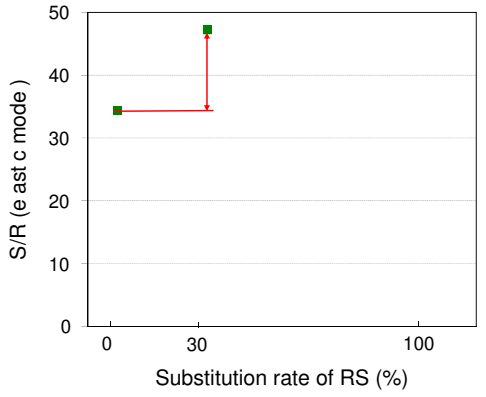

Fig. 25. Influence of substitution rate of RS on cracking sensitivity.

4. Conclusions

The study presented in this paper focused on the plastic shrink age and cracking sensitivity of concrete at early age. Experimental results, related to the effect of the rate of water saturation and sub stitution of recycled aggregates, were presented. Moreover, an esti mation of a potential early age cracking sensitivity based on a stress/strength elastic approach was also developed, focusing on the evolution of elastic properties and plastic shrinkage. A model allowing the prediction of the elastic parameters based on the

evolution of the hydration degree was established. Based on the results presented in this paper the following conclusions can be drawn:

- A timeline was established for a better understanding of the evolution of plastic shrinkage by showing correlations with the evolution of other properties at early age. For instance, the shear modulus G allows deducing the influence of other early age parameters. The thresholds $G = 0.33$ GPa and 2.7 GPa were actually proposed to easily determine initial and final setting respectively, based on the ultrasonic measurements.
- The initial water saturation of recycled aggregates varied but the added water content was adjusted in order to keep the the oretical effective water content (W_{eff}) constant. Four concrete mixtures were deduced by varying only the initial water satura tion of gravel, expressed as a percentage of saturated surface dried (SSD) state: at natural moisture (30SSD), partially satu rated (70SSD), totally saturated (100SSD) and over saturated (120SSD). This resulted in minor changes in concrete behaviour. Only two hours after casting the concrete, the water saturation of the recycled gravel had actually reached 90%. As a conse quence, the initial water saturation had a relatively weak effect on plastic shrinkage of recycled aggregates concrete.
- The rate of substitution of recycled gravel had a relatively low influence on plastic shrinkage. The concrete mixtures were actually designed keeping the maximum paste thickness (MPT) constant.
- The concrete with 30% recycled sand showed the highest plastic shrinkage. Recycled sand actually develops a significant surface area, especially at the level of fines. The effective water intended for the cement paste is attracted and kept by the recy cled fines, which results in higher plastic shrinkage related to insufficient curing.
- A model was proposed to represent the evolution of the Young modulus as a function of the hydration degree. A good correla tion was found for all the mixtures studied in this study. Addi tional tests would be necessary to generalize this simple equation for concrete with different rates of substitution and W_{eff}/Cement ratios.
- The cracking sensitivity at early age was assessed according to an experimental approach. This was based on experimentally assessed tensile strength and stresses calculated from plastic shrinkage and elastic modulus. The proportion of recycled aggregates was a more influencing parameter than initial water saturation.
- The cracking sensitivity is not proportional to the recycled aggregate content. The concrete mixtures with 30% recycled gravel and sand were characterized by a higher stress develop ment due to the fast increase of elastic modulus and early age deformation respectively which implied higher cracking sensitivity.

From the experimental analyses performed in this study, it seems possible to design concrete mixtures with significant pro portions of recycled coarse aggregates while keeping the cracking sensitivity at the level of conventional concrete. It is recommended to over saturate aggregate and to avoid using the finest particles.

Acknowledgments

Support from the Agence Nationale de la Recherche (ANR) (National Research Agency, France) is acknowledged (ECOREB pro ject). The authors would like to thank UNPG (National Association of Aggregate Producers, France) for providing some of the aggregates.

References

[1] F. Krausmann, S. Gingrich, N. Eisenmenger, K.-H. Erb, H. Haberl, M. Fischer-Kowalski, Growth in global materials use, GDP and population during the 20th century, Ecol. Econ. 68 (10) (2009) 2696–2705.
[2] M. Fischer-Kowalski, M. Swilling, E.U. von Weizsäcker, Y. Ren, Y. Moriguchi, W. Crane, F. Krausmann, N. Eisenmenger, S. Giljum, P. Hennicke, P. Romero Lankao, A. Siriban Manalang, S. Sewerin, Decoupling natural resource use and environmental impacts from economic growth, A Report of the Working Group on Decoupling to the International Resource Panel, UNEP, 2011.
[3] PN-RECYBETON, RECYBETON: RECYclage complet des BETONs, 2011. France.
[4] EEA, Effectiveness of Environmental Taxes and Charges for Managing Sand, Gravel and Rock Extraction in Selected EU Countries. EEA Report 2/2008, European Environment Agency (EEA), Copenhagen, 2008.
[5] R. Landgren, Water–vapor adsorption–desorption characteristics of selected lightweight concrete aggregates, in: Proceedings of the American Society for Testing and Materials, Philadelphia, 1964, pp. 830–845.
[6] P.B. Bamforth, Rapport CIRIA: early-age thermal crack control in concrete, 2007. p. 112.
[7] NF EN 1097-6, Tests for mechanical and physical properties of aggregates—Part 6: determination of particle density and water absorption, 2001.
[8] T. Powers, Properties of Fresh Concrete, John Wiley, London, 1968.
[9] E. Roziere, R. Cortas, A. Loukili, Tensile behaviour of early age concrete: new methods of investigation, Cem. Concr. Compos. 55 (2015) 153–161.
[10] Z. Bayasi, M. McIntyre, Application of fibrillated polypropylene fibers for restraint of plastic shrinkage cracking in silica fume concrete, ACI Mater. J. 99 (4) (2002) 337–344.
[11] S. Swaddiwudhipong, H.R. Lu, T.H. Wee, Direct tension test and tensile strain capacity of concrete at early age, Cem. Concr. Res. 33 (12) (2003) 2077–2084.
[12] T.A. Hammer, K.T. Fossa, Ø. Bjøntegaard, Cracking tendency of HSC: tensile strength and self generated stress in the period of setting and early hardening, Mater. Struct. 40 (2007) 319–324.
[13] D. Ravina, R. Shalon, Plastic shrinkage cracking, ACI J. 65 (4) (1968) 282–294.
[14] Aci-209R-92, Prediction of creep, shrinkage, and temperature effects in concrete structures, 1997. Farmington Hills.
[15] E. Holt, Contribution of mixture design to chemical and autogenous shrinkage of concrete at early ages, Cem. Concr. Res. 35 (3) (2005) 464–472.
[16] A. Darquennes, M.I.A. Khokhar, E. Rozière, A. Loukili, F. Grondin, S. Staquet, Early age deformations of concrete with high content of mineral additions, Constr. Build. Mater. 25 (4) (2011) 1836–1847. Apr..
[17] A. Katz, Properties of concrete made with recycled aggregate from partially hydrated old concrete, Cem. Concr. Res. 33 (2003) 703–711.
[18] A. Domingo-Cabo, C. Lázaro, F. López-Gayarre, M.A. Serrano-López, P. Serna, J. O. Castaño-Tabares, Creep and shrinkage of recycled aggregate concrete, Constr. Build. Mater. 23 (7) (2009) 2545–2553.
[19] M. Tavakoli, P. Soroushian, Drying shrinkage behavior of recycled aggregate concrete, Concr. Int. (1996) 58–61.
[20] T. Grazia, Comportement Des Bétons Au Jeune Âge, Faculté de science et de Genie, Université Laval, 1999 (Ph.D.).
[21] R. Cortas, E. Rozière, S. Staquet, A. Hamami, A. Loukili, M.-P. Delplancke-Ogletree, Effect of the water saturation of aggregates on the shrinkage induced cracking risk of concrete at early age, Cem. Concr. Compos. 50 (2014) 1–9.
[22] S. Zhutovsky, K. Kovler, A. Bentur, Efficiency of lightweight aggregates for internal curing of high strength concrete to eliminate autogenous shrinkage, Mater. Struct. 35 (2002) 97–101.
[23] A.Z. Bendimerad, E. Roziere, A. Loukili, Combined experimental methods to assess absorption rate of natural and recycled aggregates, Mater. Struct. 48 (11) (2015) 3557–3569.
[24] NF EN 206/CN, Béton – Spécification, performance, production et confirmité – Complément national à la norme NF EN 206, 2014.
[25] P. Belin, G. Habert, M. Thiery, N. Roussel, Cement paste content and water absorption of recycled concrete coarse aggregates, Mater. Struct. (2013).
[26] V. Lédée, F. De Larrard, T. Sédran, F. Brochu, LPC n°61: Essai de compacité des fractions granulaires à la table à secousses – Mode opératoire, 2004.
[27] A. Peigney, C. Laurent, E. Flahaut, R.R. Bacsa, A. Rousset, Specific surface area of carbon nanotubes and bundles of carbon nanotubes, Carbon N. Y. 39 (4) (2001) 507–514.
[28] F. De Larrard, T. Sedran, Le logiciel BétonlabPro 3, Bulletin des Laboratoires des Ponts et Chaussées (2007).
[29] NF EN 1992-1-1, Eurocode 2: Calcul des structures en béton: Partie 1–1: Règles générales et règles pour les bâtiments, 2005.
[30] NF-EN-206-1, Concrete. Specification, performance, production and conformity, 2004.
[31] F. de Larrard, T. Sedran, Optimization of ultra-high-performance concrete by the use of a packing model, Cem. Concr. Res. 24 (6) (1994) 997–1009.
[32] P. Turcry, A. Loukili, Evaluation of plastic shrinkage cracking of self-consolidating concrete, ACI Mater. J. 103 (4) (2006) 272–279.
[33] V. Slowik, M. Schmidt, R. Fritzsch, Capillary pressure in fresh cement-based materials and identification of the air entry value, Cem. Concr. Compos. 30 (7) (2008) 557–565.
[34] A. Radocea, A new method for studying bleeding of cement paste, Cem. Concr. Res. 22 (1992) 855–868.
[35] F.H. Wittmann, On the action of capillary pressure in fresh concrete, Cem. Concr. Res. 6 (1976) 49–56.

Accepted Manuscript

[36] A. Radocea, Autogenous volume change of concrete at very early age, Mag. Concr. Res. 50 (2) (1998) 107–113.
[37] EN NF196-3, Méthodes d'essais des ciments, Partie 3: Détermination du temps de prise et de la stabilité, 2009.
[38] H.W. Reinhardt, C.U. Grosse, Continuous monitoring of setting and hardening of mortar and concrete, Constr. Build. Mater. 18 (3) (2004) 145–154.
[39] TA Instruments, Introduction à la Calorimétrie et au TAM Air, 2013.
[40] J.K. Young, Hydration of Portland cement in instructional modulus in cement science, in: Roy, Materials education Council, Materials Research Laboratory, University Park, PA. USA, 1985.
[41] T. Voigt, C.U. Grosse, Z. Sun, S.P. Shah, H.W. Reinhardt, Comparison of ultrasonic wave transmission and reflection measurements with P- and S-waves on early age mortar and concrete, Mater. Struct. 38 (8) (2005) 729–738.
[42] A. Almusallam, M. Maslehuddin, M. Abdul-Waris, M. Khan, Effect of mix proportions on plastic shrinkage cracking of concrete in hot environments, Constr. Build. Mater. 12 (1998) 353–358.
[43] F. De Larrard, A. Belloc, The influence of aggregate on the compressive strength of normal and high-strength concrete, ACI Mater. J. 94 (5) (1997) 417–426.
[44] A.Z. Bendimerad, Comportements au jeune âge et différé des bétons recyclés: influence de la saturation initiale en eau et du taux de substitution (In French, Ph.D. thesis), Ecole Centrale de Nantes, 2016.
[45] A. Darquennes, B. Espion, S. Staquet, How to assess the hydration of slag cement concretes?, Constr Build. Mater. 40 (2013) 1012–1020.
[46] G. De Schutter, L. Taerwe, Degree of hydration-based description of mechanical properties of early age concrete, Mater. Struct. 29 (6) (1996) 335–344.
[47] R. Faria, M. Azenha, J.A. Figueiras, Modelling of concrete at early ages: application to an externally restrained slab, Cem. Concr. Compos. 28 (1) (2006) 572–585.
[48] Y. Lee, S.T. Yi, M.S. Kim, J.K. Kim, Evaluation of a basic creep model with respect to autogenous shrinkage, Cem. Concr. Res. 36 (7) (2006) 1268–1278.
[49] NF EN 1992-2, Eurocode 2: Calcul des structures en béton : Partie 2: Ponts en béton – Calcul et dispositionsconstructives, 2006.

Accepted Manuscript